



**HAL**  
open science

## Interaction between dietary bioactive peptides of short length and bile salts in submicellar or micellar state

Justine Guerin, Alexandre Kriznik, Nick Ramalanjaona, Yves Le Roux,  
Jean-Michel Girardet

### ► To cite this version:

Justine Guerin, Alexandre Kriznik, Nick Ramalanjaona, Yves Le Roux, Jean-Michel Girardet. Interaction between dietary bioactive peptides of short length and bile salts in submicellar or micellar state. *Food Chemistry*, 2016, 209, pp.114-122. 10.1016/j.foodchem.2016.04.047 . hal-01474124

**HAL Id: hal-01474124**

**<https://hal.univ-lorraine.fr/hal-01474124>**

Submitted on 3 Feb 2022

**HAL** is a multi-disciplinary open access archive for the deposit and dissemination of scientific research documents, whether they are published or not. The documents may come from teaching and research institutions in France or abroad, or from public or private research centers.

L'archive ouverte pluridisciplinaire **HAL**, est destinée au dépôt et à la diffusion de documents scientifiques de niveau recherche, publiés ou non, émanant des établissements d'enseignement et de recherche français ou étrangers, des laboratoires publics ou privés.

Manuscript Number: FOODCHEM-D-15-05365R1

Title: Interaction between dietary bioactive peptides of short length and bile salts in submicellar or micellar state

Article Type: Research Article (max 7,500 words)

Keywords: bile salts; CMC; DLS; ITC; milk whey proteins; peptides; tryptophan intrinsic fluorescence

Corresponding Author: Dr. Jean-Michel Girardet,

Corresponding Author's Institution: URAFPA - PB2P

First Author: Justine Guérin

Order of Authors: Justine Guérin; Alexandre Kriznik; Nick Ramalanjaona; Yves Le Roux; Jean-Michel Girardet

Abstract: Bile salts act as steroidal detergents in the gut, which could also interact with peptides and improve their bioavailability, but according to an unclear mechanism. The occurrence of direct interaction between milk bioactive peptides, Ile-Asn-Tyr-Trp, Leu-Asp-Gln-Trp, and Leu-Gln-Lys-Trp, and different bile salts in submicellar or micellar state was investigated by intrinsic fluorescence measurement and dynamic light scattering, above the critical micellar concentration, the latter being determined by isothermal titration calorimetry. The peptides form aggregates, spontaneously. In the presence of bile salts, some released peptide monomers were bound at the micellar surface. The lack of hydrogen bond involving the C12-OH group of the steroid skeleton and the acidic function of some bile salts might promote the interaction with the peptides, as well as the lack of the C12-OH group rather than that of the C7-OH group. At submicellar concentrations, sodium taurochenodeoxycholate and taurodeoxycholate readily interacted with the most hydrophobic peptide Ile-Asn-Tyr-Trp.



Vandœuvre-lès-Nancy, March 17, 2016

**Revised submission FOODCHEM-D-15-05365**

Dear Editor,

Thank you for having revised our article entitled:

**“Interaction between dietary bioactive peptides of short length and bile salts in submicellar or micellar state”**

By Justine Guerin, Alexandre Kriznik, Nick Ramalanjaona, Yves Le Roux, Jean-Michel Girardet

We have corrected the manuscript according to the requests of the two reviewers (see the attached file ‘Answers to reviewers’). Figure S1 has been corrected according to the request of reviewer 2. Please, could you reproduce Figure 3 in color on the Web and in black-and-white in print ?

Thanking you in advance,  
Yours faithfully,

Dr. Jean-Michel GIRARDET

## Answer to Reviewers

### Reviewer #1

**This manuscript described a study on the interaction between dietary bioactive peptides of short length and bile salts in submicellar or micellar state. Although there is some scientific significance in this manuscript, there are still some issues worth considering.**

- 1. The major problem that needs attention is the lack of experiments on the molecular mechanism of some bile salts promoting the interaction with the peptides.**
- 2. After the interaction between bioactive peptides and bile salts, if the conformation of these peptides also changed, how to change?**
- 3. In fact, what I want to know is the authentic significance of this study.**
- 4. please rewrite the highlights.**

Firstly, we want to thank the reviewer for having revised our manuscript. It is important to note that this study mainly aims to describe and finally to highlight direct non-covalent interactions between short peptides of high physiological interest and pure bile salts. For this purpose, fluorescence spectroscopy and dynamic light scattering (DLS) were both combined to show that: i) pure peptides spontaneously aggregate in aqueous buffers, ii) peptide aggregates can be disrupted by some bile salts when added in the medium, iii) in some cases, the peptides seem to likely adsorb onto the surface of some bile salt micelles without disturbing their micellar structure. Obviously, some key features could be inferred from the results. However, determining the interaction mechanism of those peptide aggregates with bile salt micelles at the molecular level would deserve to be addressed to more detailed works because of the high complexity of the systems. As a starting point, NMR could be envisaged as a promising technology in identifying the molecular/functional determinants of the interaction between bile salts with those peptide aggregates. But, the NMR signature of the peptide could potentially be hidden by strong signals from the added bile salts. Alternatively, infrared spectroscopy could also help to provide information about conformational changes of the peptides, especially when they interact with bile salts. However, as shown in our study, the peptides formed aggregates in aqueous buffers, so that any significant changes in the infrared spectra could also involve disruption of the peptide aggregates by bile salts. More alternative strategies or approaches should thus be considered in order to go further towards molecular mechanisms.

Finally, for a clearer presentation of our study, the highlights were rewritten as required by the reviewer.

### Reviewer #2

**The paper is well written and results support the claims. Bile salts are one of the most studied among several compounds used to enhance nasal absorption. Kramer et al., 1994 have described how the attachment of a peptide to the C3 position of the bile acid increases uptake of the peptide. Given their importance, the development of accurate**

**and sensitive methods of instrumental analysis has been the subject of intensive research.**

We thank the reviewer for the correction of the manuscript and for his/her good advices.

Page 3, lines 62-64: Indeed, the study of Kramer et al. (1994) seems to us very interesting and is quoted in the “Introduction” section of the revised version as following: “On the other hand, Kramer et al. (1994) have described how the covalent attachment of peptide to bile salt increases uptake of the peptide by ileal brush-border membrane vesicles via the specific intestinal absorption pathway for bile acids.”

Page 21, lines 536-538: Reference Kramer et al. (1994) is added in the “References” section.

### **Minor comments:**

#### **- Table 3:**

**Particle sizes, all the 3 peptides (INYW, LDQW, LQKW) are following the similar trend in all bile salts except LDQW in NaTDC. Can the authors explain the discrepancy?**

Indeed, it was a wrong value of particle size and we apologize to the reviewer. We have repeated this measurement in the same conditions as before and corrected the value (particle size of 3.8 nm instead of 5.1 nm) on Table 3 and the curve obtained with a mixture of LDQW and NaTDC on Figure S1 (supplementary data).

#### **- DLS measurements:**

**1. Each sample should be measured twice, once with the attenuator position automatically optimized for determination of size distributions and a second time with maximum open attenuator position to ensure comparability of total scattering intensities.**

Experiments are performed with samples of low concentration which do not scatter light much. Thus, in this case the attenuator has been set on a position allowing more light to pass through the sample. Moreover, each measurement is based on 12-16 scans by the Nanosizer device, with an automated attenuator position that allows to obtain better accuracy and reproducibility, which, with all the respect addressed to the reviewer, should not be modified as recommended by Malvern (manufacturer).

**2. Did the influence of all buffer components on viscosity and Refractive index are accounted for or not?**

Concerning the refractive index, we applied on it a corrective value including the contribution of the buffer as advised by the manufacturer (values pre-implemented into the software).

**- ITC measurements:**

**A critical step in the analysis of an ITC thermogram is the distinction between the net reaction heat and the instrumental baseline power trace.**

**1. Did you carry out Automated baseline adjustment and peak integration (both pre- and post-injection baselines)?**

We carry out an automated pre-baseline adjustment. For the post-baseline, we subtracted a blank run constituted of a buffer/buffer titration, but it was an insignificant process due to the huge heat signal measured for each bile salt (around 20  $\mu\text{cal/s}$  at the maximum of the injection peak). The sentence page 7 lines 164-165 is completed by "...and a blank titration (buffer into buffer) was subtracted".

**2. Did you inject 1.4 ml sample or the 1.428 ml is the size of the cell?**

Page 7, lines 159-161: The sentence is corrected as following: "During the titration, each concentrated bile salt solution was sequentially injected into a 1.428-ml reaction cell..." (cell volume: 1.428 ml).

**3. What is reference power set on the instrument? What is the setting of the filter period?**

We set a reference power of 2  $\mu\text{cal/s}$  adapted to the huge endothermic signals and the filter period was set to 2 s allowing the software to register the entire titration process (120 min). The sentence "Reference power was set at 2  $\mu\text{cal/s}$  adapted to the huge endothermic signals and the filter period was set to 2 s." is added in the text, page 7, lines 163-164.

## Highlights

1/ Fluorescence spectroscopy and DLS were used to highlight peptide-bile salt interaction

2/ Antioxidant peptides from milk: LDQW, LQKW and INYW were studied as peptide models

3/ Self-aggregated peptides were dissociated by bile salt micelles

4/ Released peptides were likely bound to the surface of bile salt micelles

5/ INYW could especially interact with bile salts at submicellar concentrations





29

30 **ABSTRACT**

31

32 Bile salts act as steroidal detergents in the gut, which could also interact with peptides and improve  
33 their bioavailability, but according to an unclear mechanism. The occurrence of direct interaction  
34 between milk bioactive peptides, Ile-Asn-Tyr-Trp, Leu-Asp-Gln-Trp, and Leu-Gln-Lys-Trp, and  
35 different bile salts in submicellar or micellar state was investigated by intrinsic fluorescence  
36 measurement and dynamic light scattering, above the critical micellar concentration, the latter being  
37 determined by isothermal titration calorimetry. The peptides form aggregates, spontaneously. In the  
38 presence of bile salts, some released peptide monomers were bound at the micellar surface. The  
39 lack of hydrogen bond involving the C12-OH group of the steroid skeleton and the acidic function  
40 of some bile salts might promote the interaction with the peptides, as well as the lack of the C12-  
41 OH group rather than that of the C7-OH group. At submicellar concentrations, sodium  
42 taurochenodeoxycholate and taurodeoxycholate readily interacted with the most hydrophobic  
43 peptide Ile-Asn-Tyr-Trp.

44

45

46 *Keywords:* bile salts, CMC, DLS, ITC, milk whey proteins, peptides, tryptophan intrinsic fluores-  
47 cence

48

## 49 1. Introduction

50

51 Biological activities of peptides have been widely studied during the two last decades. Thus,  
52 several milk-derived bioactive peptides are nowadays commercially available in functional foods  
53 but also in ingredients (Mills, Ross, Hill, Fitzgerald, & Stanton, 2011). To prove their effectiveness  
54 *in vivo*, there is a growing interest in the study of the bioavailability of such dietary bioactive  
55 peptides in the gastrointestinal tract. In this context, bile salts, as steroidal detergents, may help  
56 bioactive peptides in reaching their targets in their active form during the postprandial phase in the  
57 gut. Indeed, they increase epithelial paracellular permeability by modulating tight junctions and  
58 therefore, facilitate the transport of drugs and other nutrients through the intestinal barrier  
59 (Mukaizawa et al., 2009). Cakir-Kiefer, Miclo, Balandras, Dary, Soligot, and Le Roux (2011) have  
60 shown, for instance, that the bile salts protect the  $\alpha$ -casozepine, an  $\alpha_{s1}$ -casein decapeptide exhibiting  
61 an anxiolytic activity, against hydrolysis by intestinal peptidases and also improve the transport of  
62  $\alpha$ -casozepine across Caco-2 cell monolayer. On the other hand, Kramer et al. (1994) have described  
63 how the covalent attachment of peptide to bile salt increases uptake of the peptide by ileal brush-  
64 border membrane vesicles via the specific intestinal absorption pathway for bile acids.

65 Bile salts are components derived from the cholesterol molecule which display an  
66 amphipathic complex structure: The convex side of their cyclopentanoperhydrophenanthrene  
67 nucleus (steroid skeleton) is hydrophobic, with the presence of hydrogen and methyl groups,  
68 whereas the concave side is hydrophilic due to the presence of hydroxyl groups. Bile salts also  
69 possess a lateral chain that may be conjugated with taurine or glycine (Bloch & Watkins, 1978;  
70 Maldonado-Valderrama, Wilde, Macierzanka, & Mackie, 2011). Bile salts can be categorized  
71 according to the number and position of hydroxyl groups but also to the presence or not of  
72 conjugation. Due to the spatial geometry of the steroid skeleton, the bile salts can form micelles  
73 with a low aggregation number. The morphology of these micelles is complex and still under study  
74 (e.g. Posa & Sebenji, 2014). Below the critical micellar concentration (CMC), the bile salts are in

75 monomeric form, whereas in conditions neighboring CMC, small aggregates begin to form primary  
76 micelles (Madenci & Egelhaaf, 2010). Bile salts are secreted in the liver and transported *via* the bile  
77 into the intestine, where they improve digestion, for instance, by emulsifying products from  
78 enzymatic breakdown of dietary fats by forming mixed micelles with the poorly-soluble nutrients  
79 which will be further transported through the intestinal barrier (Verde & Frenkel, 2010). They also  
80 play a major role in the enzymatic lipolysis by interacting with the colipase, an amphiphile  
81 polypeptide of 10 kDa that anchors the pancreatic lipase at the surface of lipid droplets in the  
82 intestine. The hydrophilic side of the colipase interacts with the lipase, whereas its hydrophobic side  
83 is a common binding site for lipid droplets and bile salts (Kerfelec et al., 2008).

84         The enterohepatic circulation of bile salts contributes to the regulation of cholesterol  
85 homeostasis. Many studies have reported the hypocholesterolemic effects of proteins. Peptides  
86 released by proteolysis and exhibiting high bile salt binding capacity could inhibit the reabsorption  
87 of bile salts in the ileum leading to decrease the blood cholesterol level. For instance, a  $\beta$ -  
88 lactoglobulin-derived pentapeptide (Ile<sup>71</sup>-Ile-Ala-Glu-Lys<sup>75</sup>) has been identified to have a  
89 hypocholesterolemic effect according to an unclear mechanism but likely involving bile salt binding  
90 properties (Nagaoka et al., 2001). More recently, some authors have reported the ability of peptide  
91 hydrolysates to inhibit bile salt re-absorption in the ileum, and therefore to lower cholesterol levels  
92 in the bloodstream (Perez-Galvez, Garcia-Moreno, Morales-Medina, Guadix, & Guadix, 2015).  
93 This would also be directly linked to their capacity to bind bile salts. But the interactions at  
94 molecular scale between bile salt and small peptides are still unclear.

95         Noteworthy, bile salts are also able to bind compounds such as drugs, proteins, or high-  
96 molecular mass polypeptides, for which the molecular interactions have been studied in details. For  
97 instance, interaction of phenothiazines, anxiolytic drugs, with bile salts such as sodium cholate  
98 (NaC) and sodium deoxycholate (NaDC) has been recently investigated by measurement of  
99 different physico-chemical parameters including CMC, surface tension, UV absorption, and  
100 intrinsic fluorescence emission. The results showed that these drugs can interact with these bile salts

101 to form mixed micelles, either by electrostatic interactions involving the  $(\text{CH}_3)_2\text{NH}^+$  group of the  
102 drug molecule and the carboxylate function of the lateral chain of the bile salts, or by hydrophobic  
103 interactions between the phenothiazine ring and the hydrophobic convex side of the steroid skeleton  
104 (Mahajan & Mahajan, 2012). In another study, some authors have shown that oil-in-water  
105 emulsions stabilized with either  $\beta$ -lactoglobulin or lactoferrin interact with a complex mixture of  
106 bile salts and that the interaction capability mostly depends on the isoelectric point (pI) of the  
107 proteins (Sarkar, Horne, & Singh, 2010; Singh & Sarkar, 2011). Another study using circular  
108 dichroism has unveiled interaction between bile salts (NaC and NaDC), either in submicellar or  
109 micellar forms, and polypeptides such as poly[Leu-Leu-Lys] and poly[Leu-Leu-Asp] displaying  
110 molecular masses ranging from 94 to 140 kDa (D'Alagni, D'Archivio, & Giglio, 1993). According  
111 to the authors, both NaC and NaDC may interact with the polypeptides either by hydrophobic  
112 interaction involving their hydrophobic side and the Leu residues or by forming hydrogen bonds  
113 between the hydroxyl groups located at C3 and C12 of the steroid skeleton and the amino function  
114 of the Lys residues.

115 Many short peptide sequences, that are encrypted in dietary proteins and liberated by  
116 bacterial or intestinal epithelial cell proteases, are known to play a beneficial role in human health.  
117 They display a variety of activities such as antimicrobial, antioxidative, antithrombotic,  
118 antihypertensive, anti-inflammatory, and immunomodulatory activities mainly investigated *in vitro*  
119 (Mills et al., 2011). Nevertheless, only few clinical studies have demonstrated biological effects of  
120 such dietary peptides (e.g. the antihypertensive lactotriptides Ile-Pro-Pro and Val-Pro-Pro;  
121 Boelsma & Kloek, 2009). To reach their target and exert their biological activity *in vivo*, the  
122 peptides of interest have to be (i) resistant toward hydrolysis by peptidases of the brush border, (ii)  
123 absorbed through the gastrointestinal barrier, and (iii) carried in the bloodstream in an active form  
124 and optionally across the blood-brain barrier.

125 The aim of the present study is to investigate non-covalent interactions between bioactive  
126 peptides at effective concentrations and pure bile salts at neutral pH (close to pH within both

127 jejunum and ileum) as a function of the bile salt concentration, then to try to define whether such  
128 interactions are rather polar or hydrophobic. The tetrapeptides Ile-Asn-Tyr-Trp (INYW) and Leu-  
129 Asp-Gln-Trp (LDQW) derived from  $\alpha$ -lactalbumin and Leu-Gln-Lys-Trp (LQKW) from  $\beta$ -  
130 lactoglobulin after thermolysin hydrolysis were chosen as bioactive peptide models having free  
131 radical scavenging activity *in vitro* (Sadat, Cakir-Kiefer, N'Negue, Gaillard, Girardet, & Miclo,  
132 2011; Contreras, Hernandez-Ledesma, Amigo, Martin-Alvarez, & Recio, 2011). The peptide  
133 LQKW also displays an antihypertensive activity in spontaneously hypertensive rats (Hernandez-  
134 Ledesma, Miguel, Amigo, Aleixandre, & Recio, 2007). Several pure bile salts were selected  
135 according to their physicochemical properties: The primary bile salts (produced in the liver) NaC,  
136 sodium chenodeoxycholate (NaCDC), sodium glycocholate (NaGC), sodium taurocholate (NaTC),  
137 and sodium taurochenodeoxycholate (NaTCDC), and the secondary bile salts (generated by  
138 intestinal bacteria) NaDC and sodium taurodeoxycholate (NaTDC). The occurrence of electrostatic  
139 or hydrophobic interactions was studied by measurements of intrinsic fluorescence emission due to  
140 excitation of Trp residues, below and above the CMC of bile salts, and by dynamic light scattering  
141 (DLS) above the CMC. Beforehand, isothermal titration calorimetry (ITC) was performed to  
142 determine the CMCs of the bile salts under the experimental conditions used.

143

## 144 **2. Materials and methods**

145

### 146 *2.1. Peptides and bile salts*

147

148 Peptides LDQW (560.26 Da), LQKW (573.33 Da), and INYW (594.28 Da) were  
149 synthesized by Genosphere Biotechnologies (Paris, France). Purity of each peptide was further  
150 improved (final purity upper than 97%) by reversed-phase high-performance liquid chromatography  
151 as described in previous study (Sadat et al., 2011). Pure bile salt (NaC, NaCDC, NaDC, NaGC,  
152 NaTC, NaTCDC, NaTDC) were purchased from Sigma-Aldrich (St. Louis, MO, USA).

153

154 2.2. *Isothermal titration calorimetry (ITC)*

155

156 The different bile salts (at 50 mM) were solubilized in 20 mM  
157 trishydroxymethylaminomethane/HCl (Tris/HCl) buffer, pH 7.0, containing 150 mM NaCl (Tris-  
158 buffered saline or TBS). All the ITC experiments were carried out at 310 K in TBS using a VP-ITC  
159 microcalorimeter (MicroCal, Northampton, MA, USA). During the titration, each concentrated bile  
160 salt solution was sequentially injected into a 1.428-ml reaction cell, initially containing the degassed  
161 buffer, to achieve the expected final concentrations. Each injection lasted 20 s, and intervals of 180  
162 s between successive injections were applied. A rotating 290-ml micro-syringe permitted a constant  
163 stirring at a speed of 300 rpm. Reference power was set at 2  $\mu$ cal/s adapted to the huge endothermic  
164 signals and the filter period was set to 2 s. Experiments were carried out in duplicate to ensure the  
165 repeatability of the method and a blank titration (buffer into buffer) was subtracted. The  
166 experimental data were analyzed using the Origin 6.2 software provided by MicroCal.

167

168 2.3. *Spectrofluorimetry*

169

170 The analyses were carried out with a Xenius spectrofluorimeter (Safas, Monaco). Each  
171 peptide was solubilized in TBS buffer at 3.4  $\mu$ M for LQKW and LDQW, and 6.6  $\mu$ M for INYW  
172 (determined by UV absorbance measurement at 280 nm) and each bile salt (100 mM in TBS buffer,  
173 determined by weighing) was mixed with the peptide solutions as volume/volume, in a quartz  
174 cuvette with an optical path of 1 cm. The final concentrations were then of 1.7  $\mu$ M for LQKW and  
175 LDQW and 3.3  $\mu$ M for INYW in order to reach *ca.* 50% of relative value of emission intensity, or  
176 EMI, at the emission wavelength  $\lambda = 358$  nm. The bile salts were used (i) at different concentrations  
177 below and close to their CMCs previously determined and (ii) at a final concentration of 50 mM,  
178 widely upper than their respective CMCs. For total fluorescence measurements, the selected step

179 was 2 nm and the bandwidth was 10 nm. The excitation wavelength was 295 nm to selectively  
180 excite Trp residue of the peptides and the emission spectrum was recorded between 310 and 550 nm.  
181 The photomultiplier voltage was adjusted between 675 and 800 V in order to obtain a signal close to  
182 50% EMI. The measurements were carried out in duplicate, at 37 °C. The emission spectrum of  
183 each bile salt (at adequate final concentration) formed a background noise and was systematically  
184 subtracted from the emission spectrum of the corresponding peptide/bile salt mixture.

185

#### 186 *2.4. Dynamic Light Scattering (DLS)*

187

188 The particle size determination of bile salt micelles and potentially, peptide aggregates was  
189 performed by granulometry on a Zetasizer Nano-S model (Malvern Instruments, Malvern, UK).  
190 Each pure peptide was analyzed by DLS at final concentrations of 3.3 μM for INYW and 1.7 μM  
191 for LQKW and LDQW, either in TBS buffer or in ultra-pure water alone or in the presence of 0.1%  
192 trifluoroacetic acid. Each pure bile salt was also analyzed by DLS at final concentration of 50 mM  
193 in TBS buffer. Each peptide/bile salt mixture was prepared in TBS buffer, by taking the same final  
194 concentrations as above. Prior to the DLS investigations, all samples were centrifuged at 21,130 g  
195 for 30 min at 37 °C to eliminate dust or undesired particles having hydrodynamic diameter higher  
196 than 1000 nm that could interfere the measure. The supernatant of each sample was gently  
197 transferred into a quartz cuvette of 12 μl and the particle size measurements were performed in  
198 triplicate at 37 °C, with a light diffusion at 173°. The data were collected in automatic mode and  
199 analyzed using the associated software DTS version 4.2 (Malvern Instruments).

200

### 201 **3. Results and discussion**

202

#### 203 *3.1 Experimental conditions*

204

205           The Trp-containing synthetic peptides used in this study corresponded to thermolytic  
206 peptides of whey proteins ( $\alpha$ -lactalbumin and  $\beta$ -lactoglobulin) that display interesting bioactive  
207 activities: free radical scavenging activity for LDQW, LQKW and INYW but also antihypertensive  
208 activity for LQKW (Contreras et al., 2011; Sadat et al., 2011). Since they possibly interact with bile  
209 salts thanks to non-covalent interactions, those peptides are therefore interesting models to  
210 investigate the influence of bile salts on the efficiency of peptide absorption through the  
211 gastrointestinal barrier. Furthermore, the presence of tryptophan residues within their primary  
212 sequence allowed them to be used as fluorescent tool to monitor their interaction with the bile salts  
213 but also their effect on the CMCs by fluorescence spectroscopy. The peptide concentrations (1.7  $\mu$ M  
214 for LQKW and LDQW, and 3.3  $\mu$ M for INYW) were in a same order of magnitude than the  
215 reported effective concentrations of other peptides tested *in vivo*, such as the antibacterial  
216 lactoferricin detected in the upper small intestine (Kuwata et al., 2001) and the 93-123  $\beta$ -  
217 caseinopeptide involved in gut protection (Plaisancié et al., 2013).

218           In the present experimental conditions, pH, the nature of the buffering agent, the ionic  
219 strength, and the concentration of bile salts were carefully chosen. Physiologically, the micellar  
220 solubilization of lipids by bile salts occurs efficiently when the bile salts have an adequate  
221 concentration. The latter is reached only in the jejunum in which the pH was *ca.* 7.0. Besides, at  
222 neutral pH, the three peptides have different states of charge and were therefore suitable models for  
223 the present study: LDQW is negatively charged (pI = 3.80), INYW is in a zwitterionic state and  
224 displays therefore a zero net charge (pI = 5.52), and LQKW is positively charged (pI = 8.75). The  
225 Tris molecule was used as buffering agent, since it is not charged at pH 7.0 (pKa = 8.06 at 25 °C  
226 and *ca.* 7.70 at 37 °C) and thus does not interact with the peptides. In the experiments performed in  
227 the presence of bile salts in micellar form, the concentration of the bile salts was fixed at 50 mM, a  
228 concentration widely greater than their respective CMCs in order to generate secondary aggregates  
229 built from primary micelles (see below). All the experiments were performed in the presence of 150  
230 mM NaCl, as the Na<sup>+</sup> and Cl<sup>-</sup> ions (as well as other electrolytes such as K<sup>+</sup>, Ca<sup>2+</sup>, and HCO<sup>3-</sup> but in



231 a lesser extent) are secreted in the bile extract and contribute to the ionic strength in the intestinal  
232 tractus.

233

### 234 *3.2 Determination of bile salt CMCs*

235

236 Bile salts undergo a rapid dynamic association-dissociation equilibrium to form self-  
237 aggregates or micelles when their concentration reaches and exceeds CMC. Usually, CMC values of  
238 bile salts are mostly determined either in pure water or in the presence of 150 mM NaCl, at 25 °C  
239 (Fini & Roda, 1987), but the temperature as well as the ionic strength exert an influence on the  
240 micelle formation: an increase of their respective values promotes a decrease of the bile salt micelle  
241 size by minimizing the electrostatic repulsions (Maestre, Guardado, & Moya, 2014). Because self-  
242 aggregation continues to proceed with increasing concentration above CMC, the detection of the  
243 lowest concentration at which the first aggregates form, strongly depends upon the physical-  
244 chemical conditions particularly (Carey, 1985). It was thus crucial to determine the CMC of each  
245 bile salt under our experimental conditions precisely, i.e. in the presence of 150 mM NaCl, at pH  
246 7.0, and at 37 °C prior to study the possible interactions between the peptides and the bile salts in  
247 submicellar concentrations and in the vicinity of their CMC.

248 Determination of the CMCs was carried out by ITC measurements according to the method  
249 of Garidel, Hildebrand, Neubert, and Blume (2000). The second derivative of the titration isotherm  
250 gives the CMC values of the bile salts with accuracy. The CMCs of NaTDC and NaTCDC were the  
251 lowest among the bile salts investigated in the present study (CMC = 1.8 mM for NaTDC and  
252 NaTCDC; Fig. 1). This was due to their particularly pronounced amphipathic nature, as NaTDC and  
253 NaTCDC possess together the highest polar side chain (sulfonate group) and the lowest content of  
254 polar hydroxyl groups (2 OH groups at C3 and C12 of the steroid skeleton for NaTDC and at C3  
255 and C7 for NaTCDC; Table 1) leading to increase the hydrophobicity of the steroid skeleton.  
256 Generally, CMCs determined for the seven kinds of bile salts in our experimental conditions

257 remained close to those reported by several authors (Table 1). In the present study, the aggregation  
258 number ( $N_{agg}$ ) was not taken into account as a relevant parameter, since it increases with the bile salt  
259 concentration above the CMC to form bigger aggregates (Garidel et al., 2000).

260

### 261 3.3 Self-aggregation of peptides

262

263 It was worthy to note that all the three peptides were able to form aggregates in solution at  
264 neutral pH, as shown by DLS performed with the pure peptides in TBS (main particle sizes of 178,  
265 527, and 489 nm for LQKW, INYW, and LDQW, respectively; Table 2). However, the peptides in  
266 their monomeric form (less than 600 Da) were not detectable, as the DLS can measure sizes  
267 corresponding to a range of molecular masses between  $10^3$  and  $2 \times 10^7$  Da. Therefore, the proportion  
268 of molecules undergoing a spontaneous self-association remained unfortunately unknown.

269 The nature of the peptide self-association was mainly thought hydrophobic, probably  
270 involving the C-terminal Trp lateral chain, as the peptides were able to self-associate either in pure  
271 water or in the presence of 150 mM NaCl, but also under acidic conditions (0.1% trifluoroacetic  
272 acid in water at pH *ca.* 2.5) as observed for INYW for instance. However, electrostatic interactions  
273 such as salt bridge involving  $\beta$ -COO<sup>-</sup> of the Asp residue and  $\alpha$ -NH<sub>3</sub><sup>+</sup> of Leu could not be excluded  
274 in the self-association observed for LDQW. Indeed, this acidic peptide formed the biggest  
275 aggregates at neutral pH and the smallest ones at pH 2.5 compared to that observed for the other  
276 peptides in the same pH conditions. On the other hand, the most basic peptide LQKW displayed a  
277 reverse behavior as aggregates increased with a decreasing pH or in the absence of ionic strength  
278 which also suggested hydrophilic interactions.

279 Similarly, a well-known peptide aggregation phenomenon involving both electrostatic and  
280 hydrophobic forces concerns insulin. Smirnova et al. (2015) have reported that the aggregation  
281 process of insulin is pH-dependent, due to a compromise between electrostatic and hydrophobic  
282 strengths. Indeed, the inhibition of the self-assembly of insulin by arginine added to the medium at

283 pH 7 is rather due to the formation of hydrophobic interactions between the guanidinium group of  
284 Arg and aromatic residues of the native insulin molecule. At pH 8, the aromatic residues are  
285 however located at the surface of the insulin molecule that is unfolded and prone to readily self-  
286 assembly even in the presence of Arg.

287

### 288 *3.4 Interaction peptides/bile salts in submicellar state*

289

290 The pure peptides LDQW and LQKW displayed maximal fluorescence emission intensities  
291 of 56 and 62% EMI, respectively, at  $\lambda_{\max} = 358$  nm under our experimental conditions. The pure  
292 peptide INYW emitted a maximal fluorescence of 46% EMI, although its concentration was twice  
293 of those of LDQW and LQKW to reach *ca.* 50% EMI. In all cases, fluorescence quenching due to  
294 the presence of aspartic acid and glutamine residues in LDQW, glutamine and lysine residues in  
295 LQKW and asparagine and tyrosine residues in INYW could be reasonably expected according to  
296 the study provided by Chen and Barkley (1998). However, an additional loss of fluorescence  
297 intensity due to possible exciton coupling due to possible interactions between aromatic residues  
298 could also be considered in the case of INYW, as demonstrated decades ago (Kasha, 1963; Kasha,  
299 1991; Scholes & Ghiggino, 1994). This would be in a good agreement with the possible  
300 hydrophobic interaction between the aromatic lateral chains of the peptide as envisaged above.  
301 Nevertheless, since all experiments were performed with fixed amount of peptides, and since  
302 intrinsic tryptophan fluorescence are well-known to be sensitive towards changes in the  
303 environment polarity, those peptides have been chosen as fluorescent tool to report their own  
304 interaction with the bile salts but also to monitor their own effect on micelles formation. To this end,  
305 we systematically determined the fluorescence variation  $\Delta F$  as the difference between the total  
306 fluorescence emitted by the peptides in the presence of bile salts compared to that of the free  
307 peptides at  $\lambda_{\max} = 358$  nm ( $\Delta F$  is expressed in % of EMI variation).

308 The two charged peptides, LQKW and LDQW, displayed very low fluorescence variations

309 against increasing concentrations of NaC and NaCDC bile salts (Figs. 2a and 2b). Although no  
310 apparent CMCs were measured, we could not exclude that both peptides interact with the bile salts  
311 since a significant increase of their respective  $\Delta F$  values in the presence of micellar concentrations  
312 of NaC or NaCDC was observed (Figs. 3b and 3c). Altogether, these results suggested that in both  
313 cases, the peptides might delay micelles formation and therefore interact with NaC or NaCDC. At  
314 the molecular scale, salt bridges involving negative charges carried by the lateral chains of the bile  
315 salt monomers ( $\text{COO}^-$  or  $\text{SO}_3^-$ ) and the positive charges of the peptides ( $\alpha\text{-NH}_3^+$  or  $\varepsilon\text{-NH}_3^+$ ) should  
316 be considered in addition to the polar interactions within the aggregated peptides and beside  
317 hydrophobic interactions. This suggested that, in submicellar conditions, possible changes in the  
318 tryptophan environment between the aggregated forms and the bound forms of those peptides were  
319 too weak to be simply monitored by fluorescence. This might thus explain the low changes of  $\Delta F$   
320 observed for submicellar concentrations of NaC or NaCDC.

321 By contrast with LQKW and LDQW, experiments performed with the most hydrophobic  
322 peptide, INYW, clearly showed that the latter peptide interacted with the bile salts below and in the  
323 vicinity of their CMCs. Indeed, experiments performed in the presence of NaC and NaCDC, were  
324 for instance characterized by an increase of  $\Delta F$  values whereas a drop of  $\Delta F$  could be observed in  
325 the presence of NaTDC and NaTCDC. In all cases, it was thus possible to determine an apparent  
326 CMC ( $\text{CMC}_{\text{app}}$ ), *i.e.* a CMC determined in the presence of disturbing agent.  $\text{CMC}_{\text{app}}$  values  
327 obtained with NaC and NaCDC were comparable to that obtained for free NaC and NaCDC. On the  
328 other hand,  $\text{CMC}_{\text{app}}$  values of NaTDC and NaTCDC obtained in the presence of INYW were about  
329 four fold higher than those measured in the absence of the peptide. Although satisfying, these  
330 results also showed that the bile salts interacted differently with INYW according to their  
331 conjugation state. Indeed, in experiments performed with NaC or NaCDC, the interaction with the  
332 peptide was associated with an increase of the  $\Delta F$  values. This would suggest that those  
333 unconjugated bile salts (whatever the number of hydroxyl groups carried by the steroid skeleton)  
334 would be able to disrupt peptide aggregation leading thus to the recovery of the peptide

335 fluorescence thanks to the loss of the exciton coupling assumed to be associated with the  
336 hydrophobic self-association of the peptide. Nevertheless, the disruption of the peptide aggregates  
337 seemed neither to disturb the micellar process nor the respective structures of the primary bile salt  
338 micelles.

339 On the other hand, it is thought that INYW rather used hydrophobic interactions to bind  
340 NaTDC or NaTCDC. Indeed, the loss of the fluorescence intensity observed could be explained by  
341 a direct uptake of the peptide aggregates by the bile salts during the early micellar process leading  
342 thus to a simple fluorescence quenching. Although this assumption required further investigations to  
343 be asserted, hydrophobic interactions between the peptide and those conjugated bile salts would be  
344 in an agreement with a disturbance of primary micelles formation, since NaTDC and NaTCDC are  
345 the two most tensioactive bile salts and because these latter need a high number of monomers for  
346 hydrophobic self-assembling ( $N_{\text{agg}} = 18$  and  $22$  for NaTCDC and NaTDC, respectively; Table 1).

347

### 348 *3.5 Interaction peptides/bile salt micelles*

349

350 The total fluorescence emission variations ( $\Delta F$ ) of each peptide were determined at  $\lambda_{\text{max}} =$   
351  $358 \pm 1$  nm ( $\lambda_{\text{max}}$  slightly varied depending on the polarity of the local environment) from the  
352 emission spectra performed in the presence of bile salts at micellar concentrations. In all cases, the  
353 results clearly showed that all peptides interacted with the micelles formed from the bile salts  
354 previously used but also with those from NaDC, NaGC, NaTC, since significant changes of  $\Delta F$   
355 values upon the addition of the bile salts were observed. The use of several kinds of bile salts  
356 provided an interesting range of different structures useful to better define the importance of some  
357 chemical groups in the interaction between the peptides and the bile salt micelles.

358 Experiments carried out in the presence of NaC, NaCDC, NaDC, NaGC, and NaTC were  
359 generally associated with an increase of the maximal intensity of fluorescence emission ( $\Delta F$  from 7  
360 to 56%; Table 3) compared to that observed with the peptide alone. On the other hand, interaction

361 involving NaTDC and NaTCDC with those peptides led to a drop of  $\Delta F$  values (Table 3 and Fig. 3).  
362 Discussing such results in terms of binding strength or about the nature of the interaction between  
363 the reactants is highly difficult since the fluorescence properties of the tryptophan are strongly  
364 dependent upon its direct environment. Furthermore, no significant wavelength shift of the  
365 maximum emission peak of the peptides was observed upon addition of bile salts, indicating that  
366 the interactions mainly affect the fluorescence quantum yield of the peptides. This allows us to only  
367 discuss about the nature of the peptide-micelles interaction according mainly to the exposure level  
368 of Trp towards the solvent (water) but also in some extent towards electron-deficient groups such as  
369  $-\text{COOH}$  or  $-\text{NH}_3^+$  since both factors are known to reduce tryptophan fluorescence quantum yield in  
370 some cases. Therefore, the jump of the  $\Delta F$  values observed from interaction of the peptides with  
371 micelles made from NaCDC, NaC, but also those from NaTC, NaGC and NaDC, could be roughly  
372 attributed to a lesser exposure of the tryptophan residue towards the solvent in an agreement with an  
373 increase of their fluorescence intensities. It was not excluded in this context that a part of the  
374 peptides could be incorporated within the layers of the micelles as they could also be located on the  
375 surface of the micelles (avoiding neighboring polar electron-deficient groups) or in the inner side of  
376 the micellar structure assuming that the latter were less polar than the solvent. These aspects about  
377 the interaction between the peptides and those bile salts should be further explored through further  
378 investigations, but could explain the delay suggested as regards the micelles formation discussed in  
379 Fig. 2 (at least for LQKW and LDQW).

380 By contrast, it was to note that the fluorescence of those three peptides appeared quenched  
381 by the two most powerful amphiphiles NaTCDC and NaTDC. In addition, the quenching of Trp  
382 intrinsic fluorescence was relatively important, as the  $\Delta F$  values varied from -44 to -88% according  
383 to the nature of the mixture. The bile salts are planar amphiphiles and the formation of primary  
384 micelles is due to agglomeration of hydrophobic surfaces in a back-to-back manner (Carey, 1985).  
385 As the bile salt concentration increases widely above the CMC, the primary micelles form larger  
386 self-aggregates (secondary aggregates) by association of the hydrophilic surfaces *via* formation of

387 hydrogen bonds between hydroxyl groups. According to Kawamura et al. (1989), the growth of the  
388 micelle occurs with alternating up and down orientation of the bile salt monomers, the hydrophobic  
389 side of the steroid skeleton being shielded from water. Alternatively, Campanelli, Candeloro de  
390 Santis, D'Archivio, and Giglio (1991) suggest that the association of the bile salt monomers  
391 proceeds by electrostatic bonds leading to a helical association of the bile salts with their  
392 hydrophobic sides exposed to water. Thus, in the context of NaTCDC and NaTDC micelles, the  
393 peptides should not interact with the micellar core but rather with the micellar surface through  
394 either electrostatic bonds or hydrophobic interaction in a geometry allowing Trp to be more exposed  
395 towards the solvent. As discussed for LQKW and LDQW, the specific nature of the interaction  
396 between INYW and NaTCDC or NaTDC should also be considered with care in further  
397 investigations.

398 As speculative, all of those suggestions required to take into account the nature of the  
399 hydrophilic groups of the bile salt used in a further analysis to better understand how the micelle  
400 layers could affect the quantum yield of the tryptophan of peptides. Recently, it was reported that  
401 the hydroxyl group carried by the carbon C12 of the steroid skeleton can form a hydrogen bond  
402 with the carboxylic function of the lateral chain, whereas the formation of a hydrogen bond *via* the  
403 C7-OH group is unlikely (Posa & Sebenji, 2014). Furthermore, it is well-established that the  
404 microenvironment of the C12-OH group is more hydrophobic than that of the C7-OH group (Posa,  
405 2012). The lack of hydroxyl group at C12 may thus enhance the hydrophobicity in a more important  
406 manner than the absence of hydroxyl group at C7 explaining some specific binding behavior. For  
407 instance, comparing the results obtained with NaCDC micelles to that observed for NaDC micelles  
408 might be associated to general stronger binding of the peptides to NaCDC assuming that both kinds  
409 of micelles had the same effect upon the peptide quantum yield because of an enhanced  
410 hydrophobic interaction. As another instance, NaC, NaGC, and NaDC were able to form such  
411 hydrogen bonds with the peptide, which would help as additional bond to the hypothetical  
412 hydrophobic interactions promoting thus the increase of the peptide fluorescence. By contrast, the

413 absence of the C12-OH group in NaCDC and NaTCDC or the presence of a sulfonate function  
414 instead of the carboxylate function in NaTC, NaTCDC, and NaTDC made these latter bile salts  
415 unable to form such a hydrogen bond. In the case of the taurine-conjugated bile salts, this hydrogen  
416 bond is either very weak or not available due to the particularly very acidic feature of the sulfonate  
417 function (Ueyama, Takahashi, Onoda, Okamura, & Yamamoto, 2007). To compare, the pKa values  
418 of the taurine-conjugated bile salts are 1.9 against 5.0 and 3.9 for the unconjugated and glycine-  
419 conjugated bile salts, respectively (Roba et al., 1983; Table 1). And noticeably, those bile salts  
420 showed the most important fluorescence variations, either positive (micelles of NaTC and NaCDC)  
421 or negative (micelles of NaTCDC and NaTDC) according probably to the position of the tryptophan  
422 residue during the interaction with the peptide. The absence of hydrogen bond between the steroid  
423 skeleton (at C12) and the acidic function of the lateral chain was therefore an important factor to  
424 consider in the ability of bile salts micelles to bind peptides.

425         The interactions between the peptides and the micellar bile salts also obviously depended on  
426 the hydrophilic/hydrophobic nature of the peptides. For instance, the negatively charged peptide  
427 LDQW appeared to interact more strongly with NaGC than the two other peptides ( $\Delta F = +36\%$ ;  
428 Table 3). An explanation might come from the repulsive negative charge of the Asp side chain kept  
429 at a distance the carboxylate function of the lateral chain of NaGC from the steroid skeleton and  
430 prevented the hydrogen bond with the C12-OH group by a competitive process. As another instance,  
431 in the context of LQKW/NaCDC mixture, LQKW might readily interact *via* its  $\epsilon\text{-NH}_3^+$  group with  
432 the carboxylate function of the lateral chain available at the surface of the micelle of NaCDC, as no  
433 hydrogen bond at C12 of the steroid skeleton was formed. On the other hand, formation of a salt  
434 bridge between the side chain of Lys and the taurine-conjugated bile salt micelles could not be  
435 envisaged, since the spectra obtained for the mixtures of the two other peptides with either  
436 NaTCDC or NaTDC were almost similar to those of LQKW/NaTCDC and LQKW/NaTDC,  
437 respectively.

438         To investigate if the peptides were able to bind the surface of the bile salt micelles, the



439 hydrodynamic diameter of the micelles was determined by DLS experiments in the absence and in  
440 the presence of peptides. The pure bile salts formed micelles displaying hydrodynamic diameter  
441 values comprised between 2.2 and 4.2 nm (Table 2), in good agreement with those reported (for  
442 instance, the hydrodynamic diameter for NaC micelles at 26.5 mM is 3.0 nm; Garidel, Hildebrand,  
443 Knauf, & and Blume, 2007). Due to their hydrophobic nature, the four dihydroxylated bile salts  
444 displayed the greatest micelle sizes. In the peptide/bile salt mixtures, the size of the bile salt  
445 micelles were slightly increased at the exception of the NaDC micelles (average increase of *ca.* 13%;  
446 Table 3), whereas the peptide aggregates were partly or fully disrupted (Fig. S1). By taking into  
447 account the overall results from the fluorescence experiments and DLS measurements, it was  
448 suggested that the peptides were mainly bound at the surface of the bile salt micelles. These  
449 interactions were directly observable by the DLS method, although the monomeric peptides display  
450 small molecular masses (less than 600 Da) and were in very low proportion comparatively to the  
451 bile salts (peptide/bile salt ratio of approximately 1/5000). It is however reported that a difference of  
452 only 0.5 nm of the hydrodynamic radius measured by DLS (i.e. an increase from 2.5 to 3.0 nm) is  
453 sufficient to unveil a conformational change of a protein (e.g. calmodulin) interacting with a target  
454 peptide (Papish, Tari, & Vogel, 2002). According to these authors, the DLS method offers results  
455 closely comparable to those obtained by other methods such as small-angle X-ray or neutron  
456 scattering. It was then thought that a low increase of the particle size might be attributed to the  
457 formation of mixed peptide/bile salt micelles, for which the peptides mainly cover the surface.  
458 Complementary to the results of the fluorescence measurements, the DLS results also supported the  
459 hypothesis that the absence of hydrogen bond at C12 of the steroid skeleton might be a condition to  
460 confer to bile salts good adsorption properties of peptides.

461

#### 462 **4. Conclusion**

463

464 The present study was an approach of the molecular mechanism of interaction of milk

465 protein-derived antioxidant peptides with submicellar or micellar bile salts. The interaction closely  
466 depended upon the hydrophilic-hydrophobic balance of the peptide. This work has also highlighted  
467 that the lack of the hydrogen bond involving the C12-OH group of the steroid skeleton and the  
468 acidic function of the lateral chain of some bile salts promoted the interaction between the bile salt  
469 micelles and peptides, as well as the lack of the C12-OH group rather than that of the C7-OH group.

470 The most hydrophobic bile salts, i.e. NaTDC and NaTCDC, were able to interact at  
471 submicellar concentrations with the most hydrophobic peptide studied, i.e. INYW. At concentration  
472 higher than the CMC, NaTDC and NaTCDC micelles were revealed as possible efficient  
473 dissociating agents toward peptide aggregates and were able to adsorb at the micelle surface all the  
474 peptides studied, mainly through hydrophobic bonds.

475 In the intestine, it was then difficult to predict if peptides of complex hydrolysates provided  
476 by the diet might interact with bile salts or not and, therefore, pass through the intestinal barrier by  
477 the mean of paracellular transport or transmembrane transporters (Ganapathy & Miyauchi, 2005) in  
478 order to fully exert their biological activity *in vivo*. Nevertheless, the hydrophobic peptides might be  
479 the best protected against proteolytic digestion in the gut by adsorption onto the micellar surface of  
480 the bile salts, especially those devoid of hydrogen bond at position C12 of the steroid skeleton. As  
481 such, most of the peptides exhibiting antioxidant properties are concerned, as they are often  
482 hydrophobic.

483

#### 484 **Acknowledgements**

485

486 We thank the ‘Service Commun de Biophysique Interactions Moléculaires’ (SCBIM)  
487 platform of FR3209 CNRS-UL Bioingénierie Moléculaire, Cellulaire et Thérapeutique, for ITC and  
488 DLS experiments and data analysis.

489

#### 490 **References**

491

492 Bloch, C. A., & Watkins, J. B. (1978). Determination of conjugated bile acids in human bile and  
493 duodenal fluid by reverse-phase high-performance liquid chromatography. *Journal of Lipid*  
494 *Research*, 19, 510–513.

495 Boelsma, E., & Kloek, J. (2009). Lactotripeptides and antihypertensive effects: a critical review.  
496 *British Journal of Nutrition*, 101, 776–786.

497 Cakir-Kiefer, C., Miclo, L., Balandras, F., Dary, A., Soligot, C., & Le Roux, Y. (2011). Transport  
498 across Caco-2 cell monolayer and sensitivity to hydrolysis of two anxiolytic peptides from  
499  $\alpha_{s1}$ -casein,  $\alpha$ -caseozepine, and  $\alpha_{s1}$ -casein-f91–97: effect of bile salts. *Journal of Agricultural*  
500 *and Food Chemistry*, 59, 11956–11965.

501 Campanelli, A.R., Candeloro de Santis, S., D'Archivio, A. A., & Giglio, E. (1991). Cristal  
502 structures of bile salts: Sodium taurocholate. *Journal of Inclusion Phenomena and*  
503 *Molecular Recognition in Chemistry*, 11, 247–256.

504 Carey, M. C. (1985). Physical-chemical properties of bile acids and their salts. In H. Danielsson & J.  
505 Sjövall (Eds.), *Sterols and Bile Acids* (pp. 345–397). Amsterdam: Elsevier Science (The  
506 Netherlands).

507 Chen, Y., & Barkley, M. D. (1998). Toward understanding tryptophan fluorescence in proteins.  
508 *Biochemistry*, 37, 9976–9982.

509 Contreras, M. d. M., Hernandez-Ledesma, B., Amigo, L., Martin-Alvarez, P. J., & Recio, I. (2011).  
510 Production of antioxidant hydrolyzates from a whey protein concentrate with thermolysin:  
511 Optimization by response surface methodology. *LWT - Food Science and Technology*, 44,  
512 9–15.

513 D'Alagni, M., D'Archivio, A. A., & Giglio, E. (1993). On the interaction of polypeptides with bile  
514 salts or bilirubin-IX $\alpha$ . *Biopolymers*, 33, 1553–1565.

515 Fini, A., & Roda, A. (1987). Chemical properties of bile acids. IV. Acidity constants of glycine-  
516 conjugated bile acids. *Journal of Lipid Research*, 28, 755–759.

- 517 Ganapathy, V., & Miyauchi, S. (2005). Transport systems for opioid peptides in mammalian tissues.  
518 *The AAPS Journal*, 7, E852–E856.
- 519 Garidel, P., Hildebrand, A., Neubert, R., & Blume, A. (2000). Thermodynamic characterization of  
520 bile salt aggregation as a function of temperature and ionic strength using isothermal  
521 titration calorimetry. *Langmuir*, 16, 5267–5275.
- 522 Garidel, P., Hildebrand, A., Knauf, K., & Blume, A. (2007). Membranolytic activity of bile salts:  
523 Influence of biological membrane properties and composition. *Molecules*, 12, 2292–2326.
- 524 Hernandez-Ledesma, B., Miguel, M., Amigo, L., Aleixandre, M. A., & Recio, I. (2007). Effect of  
525 simulated gastrointestinal digestion on the antihypertensive properties of synthetic  $\beta$ -  
526 lactoglobulin peptide sequences. *Journal of Dairy Research*, 74, 336–339.
- 527 Kasha, M. (1963). Energy transfer mechanisms and the molecular exciton model for molecular  
528 aggregates. *Radiation Research*, 20, 55–71.
- 529 Kasha, M. (1991). Energy transfer, charge transfer and proton transfer in molecular composite  
530 systems. *Basic Life Science*, 58, 231–251.
- 531 Kawamura, H., Murata, Y., Yamagushi, T., Igimi, H., Tanaka, M., Sugihara, G., et al. (1989). Spin-  
532 label studies of bile salt micelles. *Journal of Physical Chemistry*, 93, 3321–3326.
- 533 Kerfelec, B., Allouche, M., Colin, D., Van Eyck, M.H., Brasseur, R., & Thomas, A. (2008).  
534 Computational study of colipase interaction with lipid droplets and bile salt micelles.  
535 *Proteins: Structure, Function and Genetics*, 73, 828–838.
- 536 Kramer, W., Wess, G., Neckermann, G., Schubert, G., Fink, J., Girbig, F., et al. (1994). Intestinal  
537 Absorption of Peptides by Coupling to Bile Acids. *Journal of Biological Chemistry*, 269,  
538 10621–10627.
- 539 Kuwata, H., Yamauchi, K., Teraguchi, S., Ushida, Y., Shimokawa, Y., Toida, T., et al. (2001).  
540 Functional fragments of ingested lactoferrin are resistant to proteolytic degradation in the  
541 gastrointestinal tract of adult rats. *Journal of Nutrition*, 131, 2121–2127.
- 542 Madenci, D., & Egelhaaf, S. U. (2010). Self-assembly in aqueous bile salt solutions. *Current*

543 *Opinion in Colloid & Interface Science*, 15, 109–115.

544 Maestre, A., Guardado, P., & Moya, M. L. (2014). Thermodynamic Study of Bile Salts  
545 Micellization. *Journal of Chemical and Engineering Data*, 59, 433–438.

546 Mahajan, S., & Mahajan, R. K. (2012). Interactions of phenothiazine drugs with bile salts:  
547 Micellization and binding studies. *Journal of Colloid and Interface Science*, 387, 194–204.

548 Maldonado-Valderrama, J., Wilde, P., Macierzanka, A., & Mackie, A. (2011). The role of bile salts  
549 in digestion. *Advances in Colloid and Interface Science*, 165, 36–46.

550 Mills, S., Ross, R. P., Hill, C., Fitzgerald, G. F., & Stanton, C. (2011). Milk intelligence: Mining  
551 milk for bioactive substances associated with human health. *International Dairy Journal*, 21,  
552 377–401.

553 Mukaizawa, F., Taniguchi, K., Miyake, M., Ogawara, K., Odomi, M., Higaki, K., et al. (2009).  
554 Novel oral absorption system containing polyamines and bile salts enhances drug transport  
555 via both transcellular and paracellular pathways across Caco-2 cell monolayers.  
556 *International Journal of Pharmacology*, 367, 103–108.

557 Nagaoka, S., Futamura, Y., Miwa, K., Awano, T., Yamauchi, K., Kanamaru, Y., et al. (2001).  
558 Identification of novel hypocholesterolemic peptides derived from bovine milk  $\beta$ -  
559 lactoglobulin. *Biochemical and Biophysical Research Communications*, 281, 11–17.

560 Papish, A. L., Tari, L. W., & Vogel, H. J. (2002). Dynamic light scattering study of calmodulin-  
561 target peptide complexes. *Biophysical Journal*, 83, 1455–1464.

562 Perez-Galvez, R., García-Moreno, P. J., Morales-Medina, R., Guadix, A., & Guadix, E. M. (2015).  
563 Bile acid binding capacity of fish protein hydrolysates from discard species of the West  
564 Mediterranean Sea. *Food and Function*, 6, 1261–1267.

565 Plaisancié, P., Claustre, J., Estienne, M, Henry, G, Boutrou, R, Paquet, A, et al. (2013). A novel  
566 bioactive peptide from yoghurts modulates expression of the gel-forming MUC2 mucin as  
567 well as population of goblet cells and Paneth cells along the small intestine. *Journal of*  
568 *Nutritional Biochemistry*, 24, 213–221.

569 Posa, M. (2012). Hydrophobicity and self-association of bile acids with a special emphasis on oxo  
570 derivatives of 5- $\beta$ -cholanic acid. *Current Organic Chemistry*, 16, 1876–1904.

571 Posa, M., & Sebenji, A. (2014). determination of number-average aggregation numbers of bile salts  
572 micelles with a special emphasis on their oxo derivatives - The effect of the steroid skeleton.  
573 *Biochimica et Biophysica Acta*, 1840, 1072–1082.

574 Roda, A., Hofmann, A. F., & Mysels, K. J. (1983). The influence of bile salt structure on self-  
575 association in aqueous solutions. *Journal of Biological Chemistry*, 258, 6362–6370.

576 Sadat, L., Cakir-Kiefer, C., N'Negue, M.-A., Gaillard, J.-L., Girardet, J.-M., & Miclo, L. (2011).  
577 Isolation and identification of antioxidative peptides from bovine  $\alpha$ -lactalbumin.  
578 *International Dairy Journal*, 21, 214–221.

579 Sarkar, A., Horne, D. S., & Singh, H. (2010). Interactions of milk protein-stabilized oil-in-water  
580 emulsions with bile salts in a simulated upper intestinal model. *Food Hydrocolloids*, 24,  
581 142–151.

582 Scholes, D. S., & Ghiggino, K. P. (1994). Electronic interactions and interchromophore excitation  
583 transfer. *Journal of Physical Chemistry*, 98, 4580–4590.

584 Singh, H., & Sarkar, A. (2011). Behaviour of protein-stabilised emulsions under various  
585 physiological conditions. *Advances in Colloid and Interface Science*, 165, 47–57.

586 Smirnova, E., Safenkova, I., Stein-Margolina, V., Shubin, V., Polshakov, V., & Gurvits, B. (2015).  
587 pH-responsive modulation of insulin aggregation and structural transformation of the  
588 aggregates. *Biochimie*, 109, 49–59.

589 Stevens, R. D., Lack, L., Collins, R. H., Meyers, W. C., Jr., & Killenberg, P. G. (1989). Effects of  
590 monosulfate esters of taurochenodeoxycholate on bile flow and biliary lipids in hamsters.  
591 *Journal of Lipid Research*, 30, 673–679.

592 Ueyama, N., Takahashi, K., Onoda, A., Okamura, T., & Yamamoto, H. (2007). Inorganic-  
593 organiccalcium carbonate composite of synthetic polymer ligands with an intramolecular  
594  $\text{NH}\cdots\text{O}$  hydrogen bond. In K. Naka (Ed.), *Biomineralization II: Mineralization Using*

595            *Synthetic Polymers and Templates* (pp. 155–194). Springer-Verlag Berlin Heidelberg  
596            (Germany).

597    Verde, A. V., & Frenkel, D. (2010). Simulation study of micelle formation by bile salts. *Soft Matter*,  
598            6, 3815–3825.

599

## Legends to Figures

**Fig. 1.** Titration isotherms of (a) sodium taurodeoxycholate (NaTDC) and (b) sodium taurochenodeoxycholate (NaTCDC) determined by isothermal titration calorimetry (ITC). The critical micellar concentration (CMC) corresponds to the  $x$ -intercept of the second derivative (in insets).  $C$ , bile salt concentration;  $H$ , enthalpy.

**Fig. 2.** Total fluorescence emission variation ( $\Delta F$  at  $\lambda_{\max} = 358$  nm) of INYW (3.3  $\mu\text{M}$ ; squares), LQKW (1.7  $\mu\text{M}$ ; triangles), and LDQW (1.7  $\mu\text{M}$ ; circles) in the presence of bile salts at submicellar concentration and in the vicinity of the CMC. (a) Sodium cholate (NaC), (b) sodium chenodeoxycholate (NaCDC), (c) sodium taurodeoxycholate (NaTDC), and (d) sodium taurochenodeoxycholate (NaTCDC). Apparent critical micellar concentration ( $\text{CMC}_{\text{app}}$ ) was defined as the intersection point between the tangent at the inflection point and the slant asymptote at high values of concentrations as shown by dashed lines on the graphs.

**Fig. 3.** Total fluorescence emission spectra ( $\Delta F$  at  $\lambda_{\max} = 358 \pm 2$  nm) of (a) INYW (3.3  $\mu\text{M}$ ), (b) LQKW (1.7  $\mu\text{M}$ ), and (c) LDQW (1.7  $\mu\text{M}$ ) in the presence of bile salts at 50 mM. NaC, sodium cholate, NaCDC, sodium chenodeoxycholate, NaDC, sodium deoxycholate, NaGC, sodium glycocholate, NaTC, sodium taurocholate, NaTCDC, sodium taurochenodeoxycholate, and NaTDC, sodium taurodeoxycholate.

### Supplementary data:

**Fig. 1S.** Hydrodynamic diameters of peptides/bile salt micelles determined by dynamic light scattering (DLS). The different bile salts (50 mM) and the peptides (a) INYW (3.3  $\mu\text{M}$ ), (b) LQKW (1.7  $\mu\text{M}$ ), and (c) LDQW (1.7  $\mu\text{M}$ ) were mixed in TBS buffer. The particle size distribution of pure peptides is represented in blue, of pure bile salts in green, and of the peptide/bile salt mixture in red.



**Table 1**

Isothermal titration calorimetry (ITC) determination of the critical micellar concentration (CMC) of bile salts in the presence of 150 mM NaCl. This table also regroups different physicochemical parameters such as the position of hydroxyl functions on the steroid skeleton, the molecular mass (MM), the pKa, the reported CMC in pure water or in the presence of 150 mM NaCl, and the reported aggregation number ( $N_{agg}$ ) in the presence of 150 mM NaCl.

Bile salt	Hydroxyl group position	MM (Da)	pKa <sup>a</sup> ( $\pm 0,1$ )	CMC (mM)		$N_{agg}$ <sup>e</sup> (150 mM Na <sup>+</sup> , pH ca. 8 and 25 °C)
				Water <sup>b</sup>	150 mM Na <sup>+</sup> <sup>c</sup>	
Primary bile salt						
NaC	3 $\alpha$ 7 $\alpha$ 12 $\alpha$	430.60	5.0	13	9.9 (11 <sup>b</sup> )	3 $\pm$ 1
NaCDC	3 $\alpha$ 7 $\alpha$	414.60	5.0	9	5.4 (4 <sup>b</sup> )	8 $\pm$ 3
NaGC	3 $\alpha$ 7 $\alpha$ 12 $\alpha$	487.60	3.9	12	8.5 (10 <sup>b</sup> )	6 $\pm$ 2
NaTC	3 $\alpha$ 7 $\alpha$ 12 $\alpha$	537.69	1.9	10	8.5 (6 <sup>b</sup> )	5 $\pm$ 3
NaTCDC	3 $\alpha$ 7 $\alpha$	521.69	1.9	2.5-3.0	1.8 (2.1 <sup>d</sup> )	18 $\pm$ 2
Secondary bile salt						
NaDC	3 $\alpha$ 12 $\alpha$	414.60	5.0	10	4.0 (3 <sup>b</sup> )	15 $\pm$ 3
NaTDC	3 $\alpha$ 12 $\alpha$	521.70	1.9	1-4	1.8 (2.0 <sup>e</sup> )	22 $\pm$ 3

<sup>a</sup>From Roda et al. (1983).

<sup>b</sup>From Fini & Roda (1987).

<sup>c</sup>Determination of the CMC by ITC in the present study.

<sup>d</sup>From Stevens et al. (1989).

<sup>e</sup>From Carey (1985).

**Table 2**

Main particle sizes of peptides solubilized in different media and of bile salts in TBS buffer determined by dynamic light scattering (DLS). The standard deviation was  $\pm 2\%$  ( $n = 3$ ).

Peptide or bile salt	TBS		Ultra-pure water		0.1% trifluoroacetic acid in water	
	Particle size (nm)	Proportion (%)	Particle size (nm)	Proportion (%)	Particle size (nm)	Proportion (%)
INYW	527	73	535	80	392	100
LQKW	178	45	400	90	544	84
LDQW	489	63	490	100	382	89
NaC	2.5	68	-	-	-	-
NaCDC	3.4	60	-	-	-	-
NaDC	4.2	65	-	-	-	-
NaGC	2.3	84	-	-	-	-
NaTC	2.2	93	-	-	-	-
NaTCDC	3.4	97	-	-	-	-
NaTDC	3.5	98	-	-	-	-

**Table 3**

Variation of the total fluorescence emission ( $\Delta F$ ) of peptides in the presence of bile salt micelles and particle size distribution of each peptide/bile salt mixture. Different particles of a same sample are separated by a slash symbol.

Peptide and bile salt	$\Delta F$ (%)	Particle sizes (nm)	Proportions (%)
INYW			
NaC	+ 19	<b>2.9/302</b>	90.2/7.2
NaCDC	+ 53	<b>3.6/281</b>	57.5/34.7
NaDC	+ 7	<b>4.1/385</b>	53.0/43.3
NaGC	- 5	<b>2.9</b>	100
NaTC	+ 29	<b>2.5/369</b>	66.4/32.1
NaTCDC	- 45	<b>3.7/809</b>	91.5/2.6
NaTDC	- 88	<b>3.7/306</b>	85.2/14.8
LDQW			
NaC	+ 24	<b>2.6/728</b>	90.8/3.7
NaCDC	+ 56	<b>3.7/262</b>	56.6/37.0
NaDC	+ 8	<b>4.2/308</b>	77.0/23.0
NaGC	+36	<b>2.4/760</b>	66.5/30.2
NaTC	+ 19	<b>2.4/620</b>	73.5/20.8
NaTCDC	- 54	<b>3.9</b>	98.8
<b>NaTDC</b>	<b>- 85</b>	<b>3.8/366</b>	<b>84.7/10.0</b>
LQKW			
NaC	+ 37	<b>2.7/302</b>	90.2/7.2
NaCDC	s.s.	<b>3.6/281</b>	57.5/34.7
NaDC	+ 15	<b>4.1/395</b>	53.0/43.3
NaGC	+ 15	<b>2.9</b>	100
NaTC	+ 37	<b>2.5/369</b>	66.4/32.1
NaTCDC	- 44	<b>3.7/809</b>	91.5/2.6
NaTDC	- 85	<b>3.7/306</b>	85.2/14.8

s.s., saturated signal. In bold character, main particles. The standard deviation of the particle size was  $\pm 2\%$  (n=3).

Figure 1

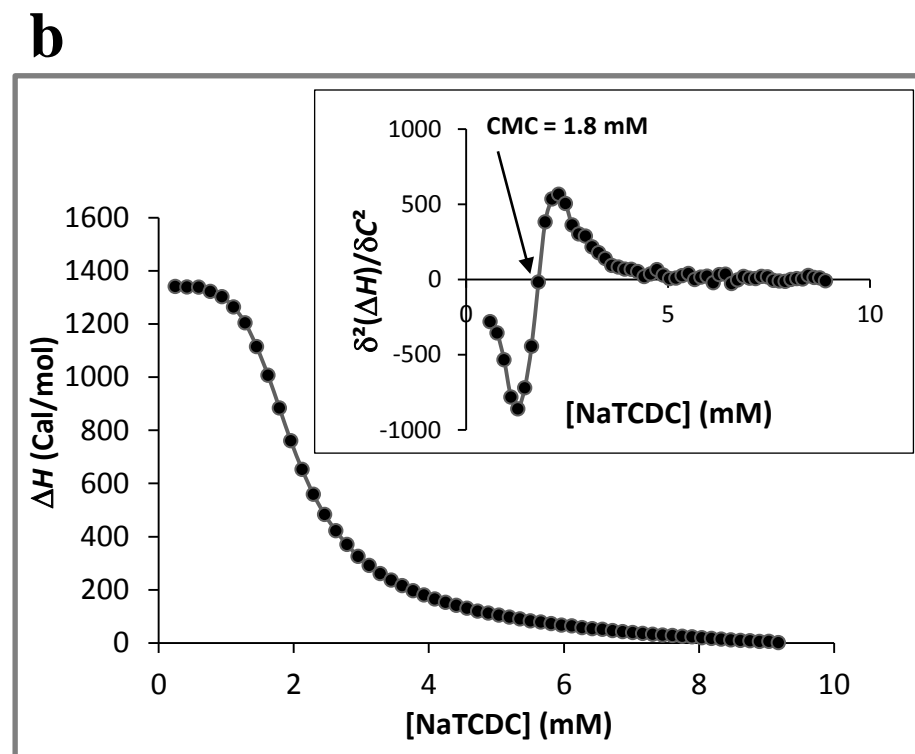
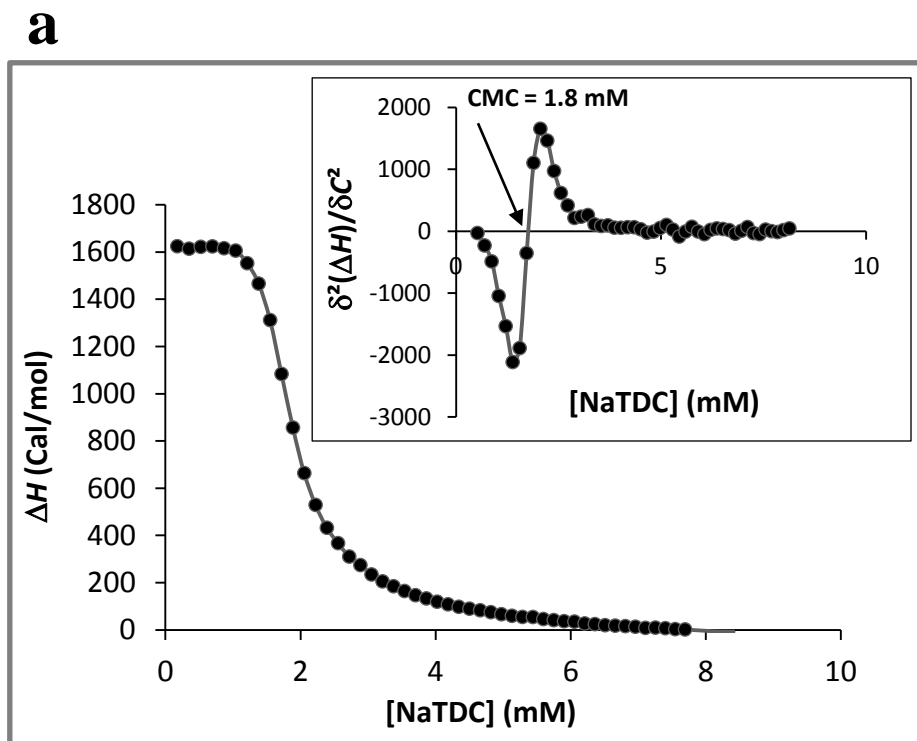


Figure 2

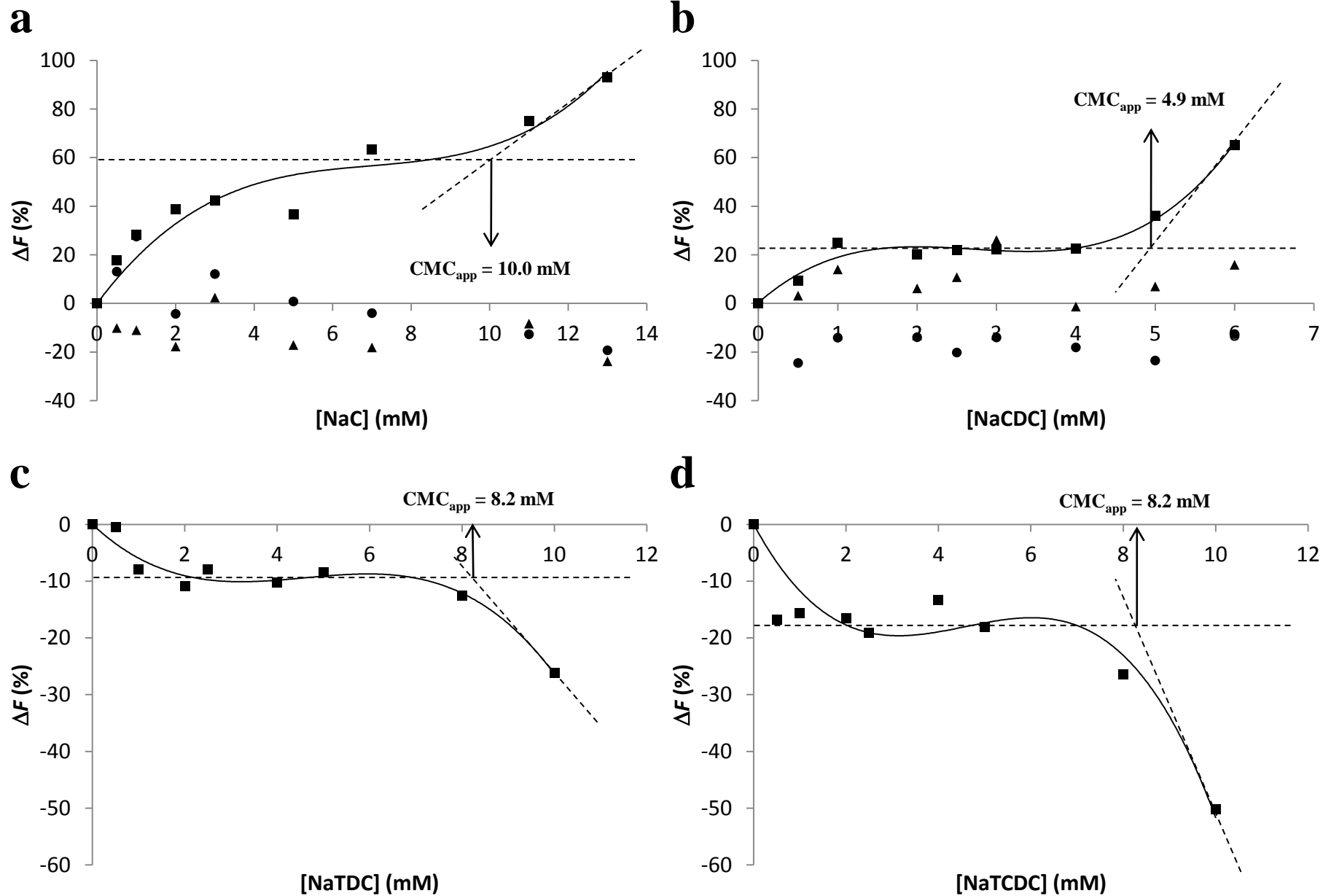


Figure 3 in color

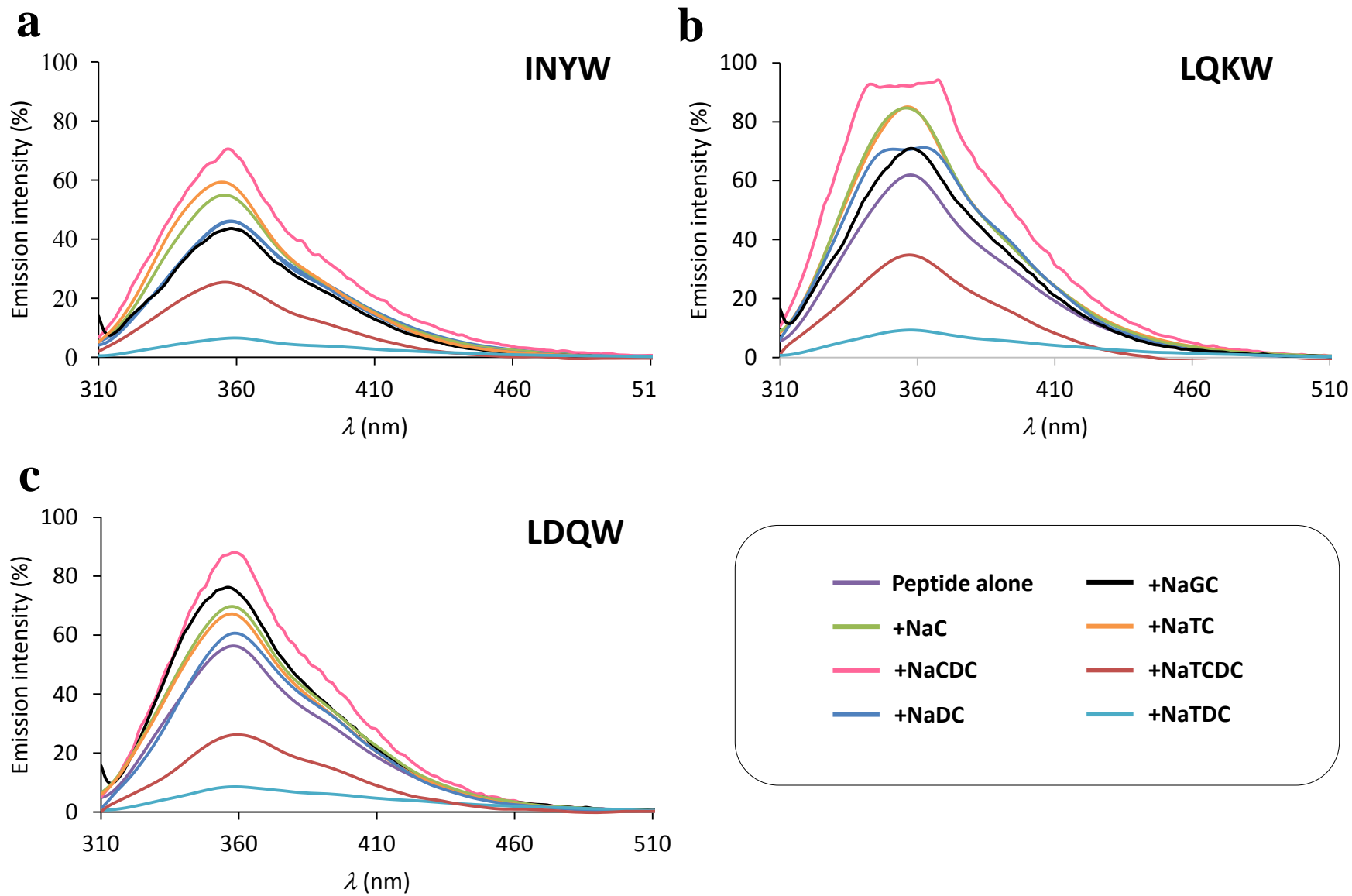
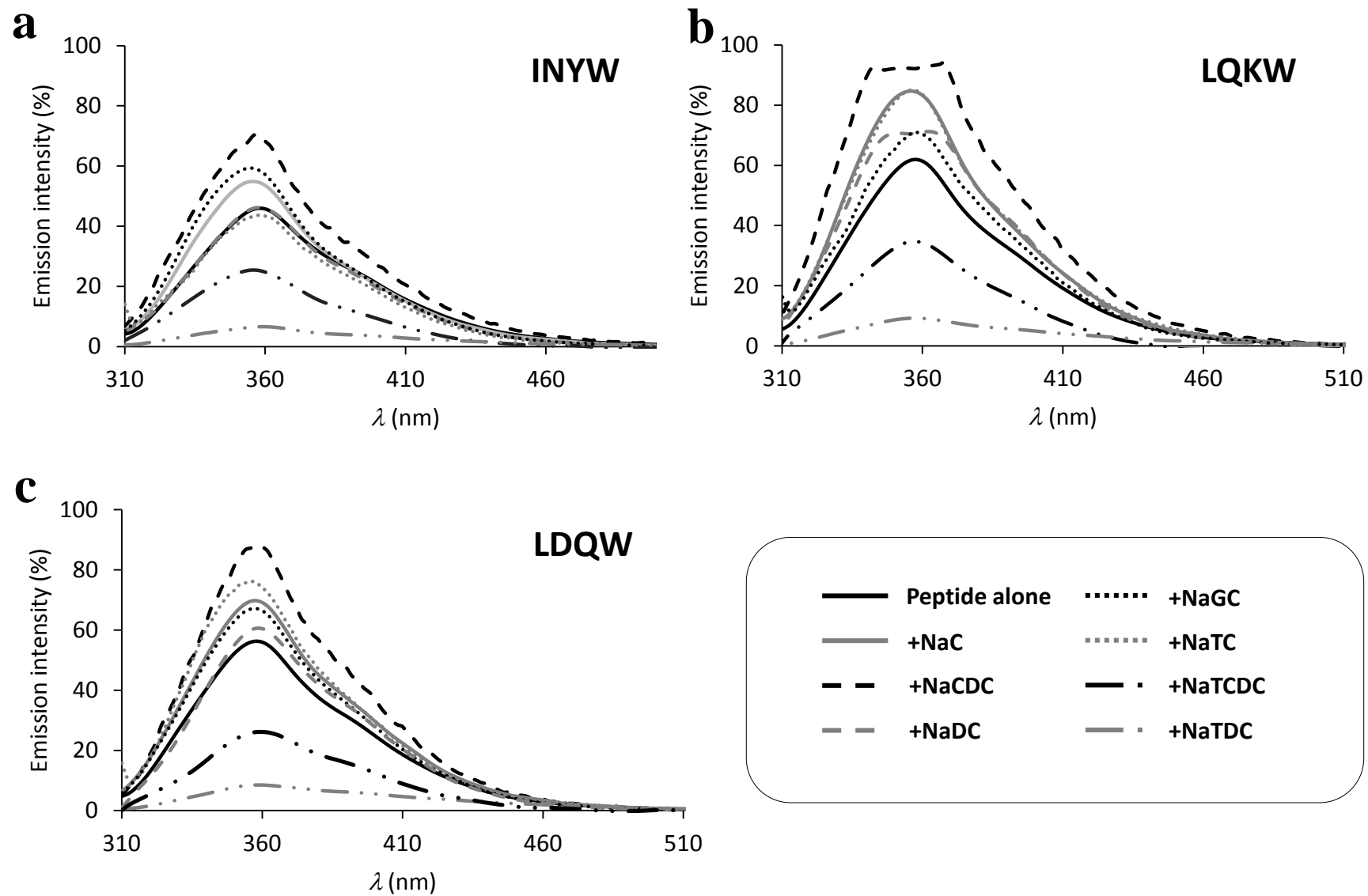


Figure 3 in black & white



**Figure S1**

[Click here to download Supplementary Material: Figure S1 revised.pptx](#)